frontiers | Frontiers in Marine Science

TYPE Original Research
PUBLISHED 04 January 2024
DOI 10.3389/fmars.2023.1208262

OPEN ACCESS

EDITED BY
Mark Meekan,
University of Western Australia, Australia

REVIEWED BY
Salvatore Siciliano,
Fundação Oswaldo Cruz (Fiocruz), Brazil
Luciana C. Ferreira,
Australian Institute of Marine Science (AIMS), Australia

*CORRESPONDENCE
Jorge Oyanadel
jorge.oyanadel@ce.ucn.cl

†These authors have contributed equally to this work

RECEIVED 18 April 2023
ACCEPTED 05 December 2023
PUBLISHED 04 January 2024

CITATION
Buchan SJ, Ramos M, Oyanadel J, Santos-Carvallo M, Bedriñana-Romano L, Valladares M, Maldonado M, Astudillo O, Sepúlveda M, Pearce S and Olavarría C (2024) Understanding the oceanographic dynamics of the Isla Chañaral baleen whale feeding ground, (Humboldt Archipelago, Northern Chile) to extend habitat protection. *Front. Mar. Sci.* 10:1208262. doi: 10.3389/fmars.2023.1208262

Understanding the oceanographic dynamics of the Isla Chañaral baleen whale feeding ground, (Humboldt Archipelago, Northern Chile) to extend habitat protection

Susannah J. Buchan[1,2,3], Marcel Ramos[1,4,5], Jorge Oyanadel[1,4*†], Macarena Santos-Carvallo[6,7†], Luis Bedriñana-Romano[2,8,9], María Valladares[1], Marinella Maldonado[10], Orlando Astudillo[1], Maritza Sepúlveda[6,7], Steve Pearce[11] and Carlos Olavarría[1,7]

[1]Centro de Estudios Avanzados en Zonas Áridas (CEAZA), La Serena, Chile, [2]Center for Oceanographic Research COPAS COASTAL, Universidad de Concepción, Concepción, Chile, [3]Departamento de Oceanografía, Facultad de Ciencias Naturales y Oceanográficas, Universidad de Concepción, Concepción, Chile, [4]Departamento de Biología Marina, Facultad de Ciencias del Mar, Universidad Católica del Norte, Coquimbo, Chile, [5]Centro de Ecología y Manejo Sustentable de Islas Oceánicas (ESMOI), Departamento de Biología Marina, Facultad de Ciencias del Mar, Universidad Católica del Norte, Coquimbo, Chile, [6]Centro de Investigación y Gestión de Recursos Naturales (CIGREN), Instituto de Biología, Facultad de Ciencias, Universidad de Valparaíso, Valparaíso, Chile, [7]Centro de Investigación Eutropia, Santiago, Chile, [8]Instituto de Ciencias Marinas y Limnológicas, Facultad de Ciencias, Universidad Austral de Chile, Valdivia, Chile, [9]Non Governmental Organization (NGO) Centro Ballena Azul, Valdivia, Chile, [10]Corporacion Nacional Forestal (CONAF) Atacama, Oficina caleta Chañaral de Aceituno, Copiapó, Chile, [11]ASL Environmental Sciences, BC, Victoria, BC, Canada

Off Northern Chile, baleen whales use the area around Isla Chañaral as a feeding ground where they forage on euphausiids. Isla Chañaral is part of the highly productive Humboldt Archipelago (~ 28°S-29°S) within the Humboldt Current System (HCS). In this study, we seek to understand the sub-mesoscale spatial distribution of fin and blue whales and their prey around Isla Chañaral using systematic and opportunistic visual sighting data of whales and systematic acoustic backscatter data of zooplankton from an Acoustic Zooplankton and Fish Profiler (AZFP); and to examine the oceanographic dynamics of the wider Humboldt Archipelago area with remote-sensing oceanographic data. We completed a total of 512.6 km of survey effort over 20 days in 2018 and 318.3 km over 16 days in 2019 collecting systematic whale sighting and backscatter data. A total of 42 fin whales, 0 blue whales and 66 unidentified whales were sighted in 2018, and 7 fin whales, 3 blue whales and 12 unidentified whales were sighted in 2019. Observed spatial distribution of backscatter and whales was strongly associated with a bathymetric feature, i.e., the submarine canyon that curves around Isla Chañaral. Generalized Additive Models showed that fin whale presence was associated with high levels of backscatter and shallow depths similar to those of the canyon. We found that long-term average geostrophic currents form a recirculation system between 28°S and 31°S that

can transport nutrient-rich upwelled surface waters back towards the Humboldt Archipelago and contribute to high biological productivity in this area. However, in summer 2019 geostrophic flow occurred away from the coast and a warm low-productivity spring explained low backscatter and whale sightings around Isla Chañaral. The unique oceanographic features of Isla Chañaral and the Humboldt Archipelago that contribute to high concentrations of Endangered baleen whales and their prey justify the extension of the Isla Chañaral Marine Reserve to include the canyon between the mainland and the island, and the implementation of a Multiple Use Marine Protected Area for the entire Humboldt Archipelago area that explicitly protects this critical feature.

KEYWORDS

baleen whale feeding ground, zooplankton acoustic backscatter, oceanographic dynamics, Humboldt archipelago, Isla Chañaral, marine protected area

Introduction

Fin whales (*Balaenoptera physalus*) and blue whales (*Balaenoptera musculus*) are the largest animals to have ever existed on earth. Off Northern Chile, fin whales use the Humboldt Archipelago and particularly the area around Isla Chañaral as a feeding ground where they forage on euphausiids (Pérez et al., 2006; Toro et al., 2016; Sepúlveda et al., 2018; Buchan et al., 2021). Blue whales, although not sighted as frequently as fin whales, are also known to forage on the same prey type in this area (Buchan et al., 2021).

The Humboldt Archipelago (~ 28°S-29°S) lies within the Humboldt Current System (HCS), a highly productive Eastern Boundary Upwelling System (EBUS) (Daneri et al., 2000; Thiel et al., 2007; Montecino and Lange, 2009) off central-northern Chile. The large-scale oceanographic processes, which drive biological productivity associated with wind-driven coastal upwelling, are relatively well-understood in the HCS (e.g., Daneri et al., 2000; Montecino and Lange, 2009). The HCS is mainly characterized by a cold surface current that flows towards the equator, and an opposite subsurface current (Peru-Chile Undercurrent: PCUC) that flows south close to the continental slope and deep shelf. The PCUC is the source of the upwelled water that is poor in dissolved oxygen, has a low pH, and is rich in nutrients (e.g., nitrates, phosphates) that fertilize the coastal photic layer favoring primary productivity and maintaining a productive food web (Thiel et al., 2007). In addition, wind forcing in this region is dominated by the southeast Pacific subtropical anticyclone driving winds with an equatorward component near the coast, which favor upwelling and vary latitudinally and seasonally (Shaffer et al., 1999; Monteiro et al., 2011; Kämpf and Chapman, 2016). Permanent intrusions of cold water are present throughout almost the entire year, from coastal upwelling events driven by Ekman transport, with greater seasonal variability in spring. These frequent upwelling events recorded along the coast, made possible by a narrow continental shelf, a strong orographic slope and quasi-weekly wind pulses associated with atmospheric disturbances trapped in the mountain range (i.e. coastal lows) (Rutllant and Montecinos, 2002). In this sense, coastal topography and the flow over the exposed platform play an important role in upwelling zones since they allow certain bays and promontories to function as larval retention areas and allow primary producers and higher trophic levels to congregate (Largier, 2020).

The Humboldt Archipelago is a remote stretch of complex coastline with and despite great touristic and scientific interest in this area, its hydrography and coastal dynamics have been poorly studied. The sub-mesoscale oceanographic features that explain the particularly high productivity and the presence of foraging baleen whales in the Humboldt Archipelago has not been examined. It is known that mesoscale (10-100 km) and sub-mesoscale (1-10 km) oceanographic processes and environmental features, such as bathymetry (Croll et al., 2005), thermal fronts (Doniol-Valcroze et al., 2007), water masses (Buchan and Quiñones, 2016; Buchan et al., 2022) can drive local whale distribution. Adequate| understanding of the oceanography that drives the distribution of whales and their prey can provide important justification for marine habitat protection. For example, Cox et al. (2018) identify common key features of marine mammal habitats in coastal areas, which include interactions between bathymetry and tidal currents, and patterns of seasonally stratification and shelf edge upwelling.

Protection of this habitat is necessary given that the Humboldt Archipelago area has been threatened by a series of industrial projects, including the now discarded Barranquilla coal plant project, the proposed Dominga copper and iron mine and mega-port, and the already approved Cruz Grande mega-port. These mega-ports propose to open shipping lanes within this critical feeding habitat for Endangered baleen whales at a time when record numbers of ship strikes are increasing off northern Chile

(Toro et al. *In prep*). Currently, only 1 nmi around Isla Chañaral (Figure 1A) and two other islands (Isla Damas and Isla Choros) are effectively protected as Marine Reserves for fisheries, although a much larger Multiple Use Marine Protected Area (MU MPA) has recently been approved that would include the entire Humboldt Archipelago. However, it is unclear whether the Humboldt Archipelago MU MPA will explicitly exclude large industrial projects and effectively protect this whale habitat from higher levels of marine traffic.

In this study, we seek to understand the submesoscale spatial distribution of fin and blue whales and their prey around Isla Chañaral using systematic and opportunistic whale visual sighting data and zooplankton acoustic backscatter survey data; and to examine the oceanographic dynamics of the wider Humboldt Archipelago area with remote sensing oceanographic data and Acoustic Doppler Current Profiler (ADCP) data.

Methods

Systematic survey data collection of zooplankton backscatter data and whale sightings

Systematic surveys were carried out between the 23rd January and the 19th of February 2018, and between the 2nd and the 28th of February 2019. Surveys were conducted on a 10 m vessel moving at a maximum speed of 4 kn (7.41 km/h) in the area surrounding Isla Chañaral (29°02'3.61"S; 71°34'37.03"W) along track lines separated by approximately 1 nmi (Figures 1B, C). During these surveys, a side-mounted Acoustic Zooplankton and Fish Profiler (AZFP) was deployed off the side of the vessel, at approximately 1 m below the sea surface and facing down, to collect acoustic backscatter data at 38, 125, 200 and 455 kHz center frequencies.

During the AZFP survey, a team of 4 observers conducted visual surveys of whales from the bow of the vessel (elevation 1.6 m), where three observers simultaneously performed continuous scans of the horizon with the naked eye covering a 180° angle, and a fourth observer acted as data scorer. Each observer performed visual scans for no more than 1.5 hours and then took a 30-min break; observers worked for approximately 6 hours per day. For all marine mammal sightings, the following data were recorded: species (in this case, fin whale, blue whale, humpback whale (*Megaptera novaeangliae*), or unidentified baleen whale), date/time, GPS position, estimated distance from the vessel and estimate angle relative to the bow. Estimates of distance from the vessel were calibrated by taking estimates from observations of objects of known distance determined by a range finder, estimated distances were then corrected according to this calibration. Corrected distances, angle and GPS position were used to calculate whale positions. Observations were made when weather conditions provided good visibility to ensure reliable data collection, i.e., Beaufort Sea state of 3 or less, with no coastal fog or rain.

Acoustic zooplankton and fish profiler data processing and analysis

The AZFP acoustic backscatter data were converted by AZFPLink software (ASL Environmental Sciences Inc.) into comma separated value format files and then processed as a matrix using custom routines of Matlab software, which allowed estimating the related variable with volume backscattering strength (Sv, dB re 1 m^{-1}), and all others mentioned below. The Sv described as Sv_{meas} by (de Robertis and Higginbottom, 2007) (Equation 1), can be expressed as the arithmetic sum of the contributions in recorded signal by scatterers and noise namely Sv_{signal} and Sv_{noise}.

$$Sv_{meas} = 10log_{10} * (10^{(Sv_{signal}/10)} + 10^{(Sv_{noise}/10)}) \quad (1)$$

So, to correctly associate the received echo to its source, the acoustic signal was first refined by eliminating background noise, estimated according to the following equation (de Robertis and Higginbottom, 2007; Ventero et al., 2019) (Equation 2):

$$Sv_{noise} = 20log_{10} * (R) + 2 * \alpha * (R) + \text{offset} \quad (2)$$

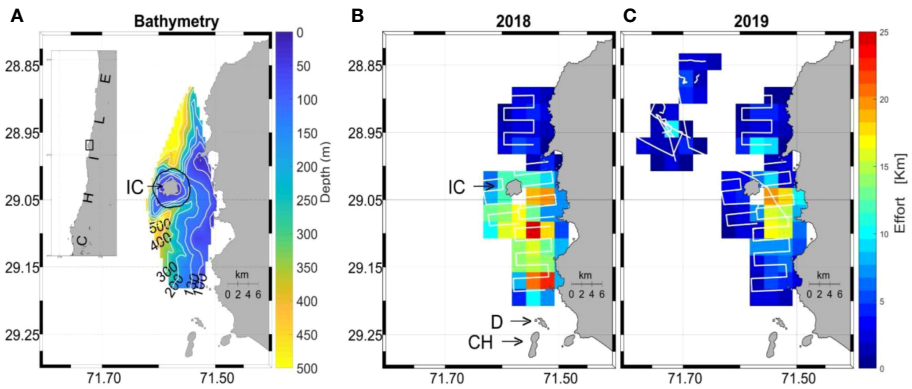

FIGURE 1
Map of study area **(A)** with bathymetry around Isla Chañaral (IC) and the Isla Chañaral Marine Reserve (black Line). Systematic survey effort is shown for 2018 **(B)** and 2019 **(C)**. Note: the two other main islands of the Humboldt Archipelago can be seen in panel **(B)**: Isla Damas (D) and Isla Choros (CH).

Where α is the absorption coefficient, R is the frequency range respective (m) and offset is the logarithmic form of sv (Equation 3):

$$\text{offset} = 10log_{10} * (sv) \quad (3)$$

The offset was determined by using the backscattering strength recorded in the space immediately below the seabed where the records are considered passive because there is no source of reflection, therefore allowing the estimation of noise values (Equation 3). For each file, an offset value was estimated using an average of at least five Sv_{meas} values selected in that area which was converted to linear form (sv), as well as the respective hourly values of the absorption coefficient.

Continuing with the array processing, acoustic records below the seafloor were eliminated from the dataset, resulting in files with only valid records from the water column. Adding to this, with the purpose of obtaining more robust integration of Sv_{signal} values, remaining effects of noise still visible in the hydroacoustic signal were eliminated. An SNR indicator was determined which reflects the contribution of noise and scatterers in the captured hydroacoustic signal, according to the methodology applied by (de Robertis and Higginbottom, 2007) (Equation 4):

$$\text{SNR} = Sv_{signal} - Sv_{noise} \quad (4)$$

A value of SNR = 3 dB was determined after a sensitivity analysis, in which it was established that this value was sufficient threshold to eliminate the remaining noise and get a greater percentage of useful data at same time. Cross-sections of all transects were reviewed to examine backscatter. Thus, from each transect, only Sv_{signal} records above this SNR threshold value were considered for subsequent analyses.

Thereafter Sv_{signal} was analyzed and first processed using a mask (data<-55 dB) to remove possible micronekton's backscatter and thus to obtain acoustic density for the 125, 200 and 455 kHz channels, by means of area backscattering coefficient (Equation 5) assessment which is defined by (MacLennan et al., 2002) as the integral of sv ($sv_{signal}(z, f)$ in this study) over a range interval $R1$ to $R2$ (i.e., $z1$ to $z2$) for each frequency (f), that is, the integrated backscatter over the entire water column of the linear form of Sv_{signal}:

$$sa = \int_{z2}^{z1} sv_{signal} dz \quad (5)$$

where sa is expressed in linear form ($m^2\ m^{-2}$) and then was converted to nautical miles called nautical area scattering coefficient ($NASC$) ($m^2\ nmi^{-2}$) (Equation 6). In this study, the range interval was from five meters above the seafloor up to five meters below the sea surface, which avoids the high reverberation in those layers.

$$NASC = 4\,\pi\,(1.852)^2 * sa \quad (6)$$

Then, $NASC$ values were transformed to a logarithmic term defined as Nautical area scattering strength (SA), expressed in dB re $1(m^2\ nmi^{-2})$ (Equation 7):

$$SA = 10\,log_{10} * NASC \quad (7)$$

In addition, simultaneous to the AZFP deployments on February 17th and 25th 2019, to confirm the presence (or absence) of acoustic signal dispersers such as zooplankton groups, diurnal plankton tows were conducted using Bongo nets (0.7 m diameter) equipped with 200 µm mesh and cod-end buckets, towed from the bottom (110 m) to the surface along a total of eleven AZFP survey transects. Also, a Nansen net (200 µm mesh) was towed vertically at five stations along survey transects.

Samples were preserved and carried at laboratory of Universidad de Valparaíso, Chile and then observed through an Olympus model S251 stereoscopic magnifying glass, up to a taxonomic resolution of specie in most of the recorded taxa. The samples were observed without a Folsom sample separator, using a Bogorov type plate and a mechanical counter to quantify the richness of taxa and abundance of organisms obtained in the different stations and sampled transects. The identification was made based on appropriate and specific literature for the zooplanktonic taxa of the coastal area of evaluation (i.e., Boltovskoy, 1981; Palma and Kaiser, 1993; Harris et al., 2000).

It should be noted that the 38 kHz channel is useful mainly for detection of large targets and air bubbles, such as fish with swim bladders (Ventero, 2016). Based on this and preliminary backscatter results, this channel was used to estimate depth since it had the longest range of the four frequencies (ASL, 2017). A sudden increase in the count value was observed at a given range due to the reflection of the signal with the seabed. For more accurate depth estimates, all gaps in the raw depth log, as well as those generated by subsequent outlier removal, were filled by interpolating from neighboring values. So, to estimate slope and roughness from the AZFP data, based on the resultant bathymetric layer, roughness (ROU) and slope (SLO) were calculated using the R package raster (Hijmans et al., 2018).

Systematic sighting generalized additive model analysis

For the statistical analysis, a grid of 500 m x 500 m grid-cell size was used to assign whales presence/absence, explanatory variables described above, and effort. Years were considered independent so this variable allocation process was conducted separately for 2018 and 2019. Fin whales and unidentified whales' sightings were combined to obtain a sufficient sample size for statistical analyses. Other species were not included in the statistical analysis because of low sample size. More than one sighting per grid-cell occurred on five occasions (8% of the presence data), because of the small number of such records we preferred to model presence/absence per grid-cell for each year instead of using a count model. On-effort track length, expressed in km, was calculated for each one of the grid-cells and for each year. To avoid extreme values in effort allocation, values below the lowest 5% of effort values (0.1 km) were replaced by this value, and a similar but inverse procedure was undertaken for the highest 1% values (5 km). Grid-cells with missing data (i.e., without effort allocation and/or AZFP backscatter data) were excluded from this analysis and the

remaining were grouped for both years to generate the final data base.

Generalized Additive Models (GAMs) were built to examine the relationships between whale occurrence and water column integrated acoustic density from the 125, 200 and 455 kHz channels as previously described. Depth, slope, and bottom roughness were also included as predictors. GAMs were built using the R package mgcv v1.8-31 (Wood, 2017). The response variable presence/absence was modeled using a binomial distribution with effort used as an offset term. Restricted maximum likelihood (REML) was used to optimize the parameter estimates and a variable selection process that uses a shrinkage approach to modify the smoothing penalty, allowing the smooth to be identically zero and to be removed from the model (Marra and Wood, 2011). Variables that had p-values > 0.05 were removed and the models were refitted to ensure that all remaining variables had p-values< 0.05 (Roberts et al., 2016; Redfern et al., 2017). Thin-plate regression splines were used for all predictors. Established metrics to compare the performance of the models were used, including Akaike's information criterion (AIC; Akaike, 1973), Akaike weights (wAIC), REML score, the percentage of explained deviance (ExpDev), the area under curve (AUC), and visual inspection of predicted densities. AUC was calculated using the R package ROCR v.1.0-11 (Sing et al., 2005). Model fit was assessed through a simulation-based approach and scaled residuals diagnostics using the R package DHARMa v. 0.4.551 (Hartig, 2022). With this package, quantile dispersion, outliers and deviation tests were implemented.

Opportunistic whale sighting data

Opportunistic whale sighting data has been compiled by the Corporación Nacional Forestal (CONAF) park service since 2015, based on reports from the fleet of 24 whale-watching boats that operate out of the village of Chañaral de Aceituno and provide whale-watching tours around Isla Chañaral during the spring and summer months. These data were analyzed to examine any possible interannual variation in whale presence off Isla Chañaral over a 5-year period (2015-2019). Opportunistic sighting data for each day during January and February were used from this database because these months are the high tourist season, and we could confidently assume that the full fleet of whale-watching boats were operating every day during these two months with negligible differences in sighting effort between both months. For both months, days with presence were determined and the monthly presence of whales (blue, fin, humpback) was calculated as the number of days with presence as a percentage of total days in the month for January and February 2015-2019. A five-year average was also calculated for monthly presence between 2015 and 2019.

Sources of bias in this citizen science dataset are probable, given that boats do not cover the study area systematically or uniformly and will often sight animals closest to port to reduce fuel costs. There is bias in reporting of species, blue whales and humpbacks are less common and arguably more charismatic than fin whales, so although there may be many fin whales in the area, when a single humpback or blue whale is present, boats will prefer these species to fin whales, which results in underreporting fin whales and overreporting blue and humpback whales. To minimize these possible biases, we preferred a presence/absence metric (monthly presence %) versus a count metric of number of sightings.

Auxiliary oceanographic data

Remote-sensing oceanographic data were obtained to interpret any possible interannual differences in whale sightings (systematic and opportunistic) and to examine the oceanographic dynamics of the wider Humboldt Archipelago area. Thus, satellite sea surface temperature (SST) and chlorophyll-a (Chla) were obtained from the MUR (Global, 0.01 degrees) product and Aqua MODIS (Global, 0.025 degrees), respectively. An average SST and Chla were obtained for the spring (November 2017 and 2018) preceding the systematic data collection in 2018 and 2019, and for the AZFP summer surveys (i.e., January 23rd to February 19th, 2018, and between February 2nd and 28th, 2019). Examining SST and Chla in November can provide information on what the upwelling-favorable conditions were like in the spring preceding the summer sampling campaigns, as November is historically the month with the strongest favorable upwelling winds (Ramos, Unpublished) which increases nutrients available for the development of phytoplankton blooms and the subsequent proliferation of zooplankton (Barlow et al., 2021).

To estimate the differences in current flow in the study area, mean geostrophic currents (from AVISO-CNES) were calculated for January and February 2018 and 2019. Moreover, mean currents obtained from a moored Acoustic Doppler Current Profiler (ADCP: RDI-Teledyne, Workhorse Sentinel, 300 kHz Model) deployed between Isla Chañaral and the mainland at 100 m depth, were also included in this analysis (Ramos, Unpublished). In this case, the mean corresponds to the depth average of the velocity vector for the same periods considered in obtaining the mean geostrophic currents. Additionally, to determine possible recirculation current systems off central-northern Chile, long-term averages (1993-2020) of geostrophic currents (from AVISO-CNES) in a meridional band between 20° and 40°S were calculated.

During the intensive campaign with the AZFP, no measurements of spatial and hydrographic currents were made around Isla Chañaral. For this reason, results from one of the few oceanographic studies with sufficient spatial coverage (with sampling resolution of ~1.5 km) around the island were used to analyze the oceanographic conditions in the area. This oceanographic study was a FIP project (Fisheries Research Fund: FIP 2006-56, Gaymer et al., 2008) carried out between January 22 and 25, 2008, in which hydrographic and current measurements were obtained around Isla Chañaral. Thus, temperature, salinity (conductivity) and pressure data were obtained with a CTD (conductivity, Temperature and Depth) Sea-Bird, model SBE 19. A total of 15 CTD stations were carried out in two zonal sections, one in the north and one in the south of the island. On the other hand, measurements of the velocity profiles of the currents were made along four transects. For this, an ADCP (RDI Workhorse Sentinel-300 KHz) with a range of 120 m

was used. The ADCP was installed on an arm at the side of the vessel (starboard) at an average depth of 1 m, the position and speed of the ship were recorded with a Garmin GPS (GPSmap 188C). The setup and acquisition of ADCP measurements were performed with the WinRiver program. The processing and analysis of the current data obtained with the ADCP (in Bottom Tracking mode) was carried out according to the protocol proposed by the manufacturer and the procedure followed by Moraga et al. (2011), and Valle-Levinson and Moraga-Opazo (2006). This includes the correction proposed by Joyce (1989) to eliminate the error of the ADCP magnetic compass with respect to the GPS direction.

Results

Spatial distribution of whales and prey backscatter

A total of 512.6 km of survey effort over 20 days in 2018 (Figure 1B) and 318.3 km over 16 days in 2019 (Figure 1C) were achieved. A total of 42 fin whales, 0 blue whales and 66 unidentified whales were sighted in 2018, and 7 fin whales, 3 blue whales and 12 unidentified whales in 2019. No humpback whales were sighted during the systematic surveys. In 2018, whales were sighted predominantly to the south of Isla Chañaral and between the island and the mainland (Figures 2A–C). In 2019, due to very low whale sightings in general around Isla Chañaral, survey effort was conducted further offshore where higher densities of fin and blue whales were eventually found (80% of total sightings that year) (Figures 2D–F), (but this offshore area was not included in the statistical modeling analysis because this area was only surveyed on 2019). In addition, there were five sightings of odontocetes in 2019: two of Risso's dolphins (*Grampus griseus*), two of pilot whales (*Globicephala* sp.) and one sighting of bottlenose dolphins (*Tursiops truncatus*).

Backscatter was much higher overall in 2018 compared with 2019 and was generally patchy, with areas of higher density to the south, to the north and in the canyon between the island and the mainland (Figure 2). Complex bathymetric features (steep slope and topographic breaks) around the island were apparent on visual inspection of the bathymetric data (Figures 1A, 3A), with a canyon that surrounds the island, starting at 500 m depth southwest of the island, shoaling to 200 m depth in the channel between the island and the mainland, and then deepening again to 500 m to the northwest of the island. In effect, the cross-section of AZFP survey data across the Isla Chañaral submarine canyon shows an example of high backscatter over a topographic break of the canyon (Figure 3A) particularly visible in 200 kHz channel (Figure 3B). At the right panels of the figure it is possible to observe swarms of zooplankton over the Isla Chañaral submarine canyon. As the frequency increases, the range decreases, so the detection of swarms is closer and appears larger in size, and the intensity of the backscatter depends on the taxonomic group.

The dominant species in the zooplankton trawls were copepods and to a lesser extent euphausiids (identified as *Euphausia mucronata*) as well as larvae of crustaceans and mollusks. This was found from both the Bongo net samples and the Nansen net samples (data not shown).

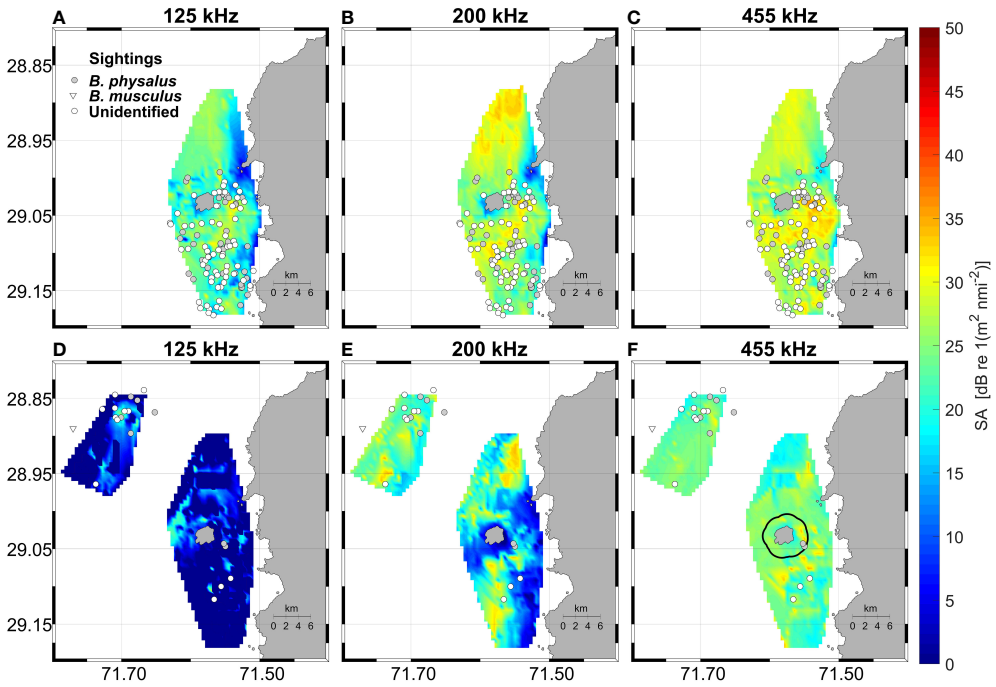

FIGURE 2
Nautical area scattering strength (SA) for the 125 kHz **(A, D)**, 200 kHz **(B, E)** and 455 kHz channels **(C, F)** and whale sightings during 2018 (upper panels) and 2019 (bottom panels). In panel **(F)** the limits of Isla Chañaral Marine Reserve (black Line) are shown. It is worth noting low sightings during 2019, and mainly further offshore to the northwest of the island.

10.3389/fmars.2023.1208262

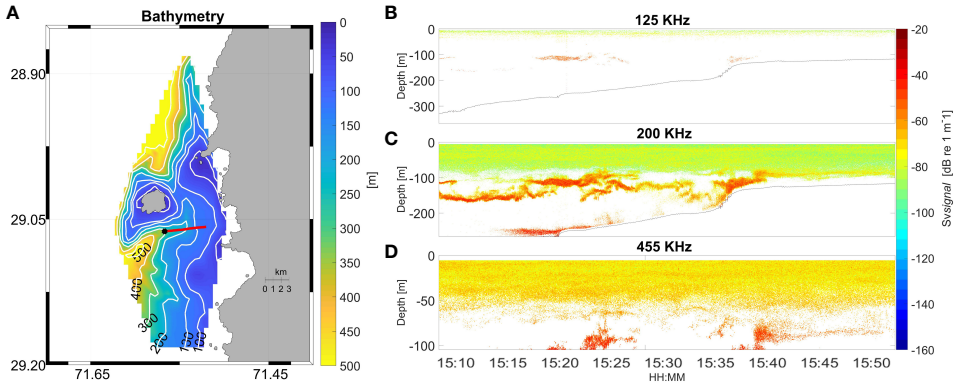

FIGURE 3
Bathymetric map of systematic survey area **(A)** with a cross-section over the canyon (red line) and start location (black dot) carried out on February 18th 2018 at 15:09 (*) on the map. Echograms of the cross-section for frequencies of 125 kHz **(B)**, 200 kHz **(C)** and 455 kHz **(D)** are shown. Seabed in panels (B) and (C) marked by solid line.

Statistical modelling of fin whale habitat

The top three ranking models all included 455 kHz backscatter, along with one other variable, i.e., depth, slope, and roughness, respectively. However, the best model clearly outperformed all other models (Table 1) and showed that whale probability of occurrence increased with increasing backscatter in the 455 kHz channel, and shallower depths (Figure 4). The 200 kHz channel also gave good model performances, although not as good as 455 kHz (Table 1). Expected versus observed residual plots using scaled residuals and tests for dispersion, outliers and deviation showed good

TABLE 1 Generalized Additive Model results and model selection based on Area Under the Curve (AUC), Deviance explained, Restricted Maximum Likelihood score (REML), Akaike's Information Criteria difference (ΔAIC), and Akaike weights (wAIC).

Model	AUC	Deviance Explained	REML	ΔAIC	wAIC
y~s(SA455)+s(depth)	0.76	9.03	184.68	0.00	0.31
y~s(SA455)+s(slope)	0.76	9.01	184.67	0.06	0.30
y~s(SA455)+s(roughness)	0.76	8.57	185.11	1.40	0.15
y~s(SA200_55)+s(slope) +s(depth)	0.76	8.29	184.32	2.22	0.10
y~s(SA200_55)+s(depth)	0.74	7.45	184.99	4.07	0.04
y~s(SA125_55)+s(slope) +s(depth)	0.76	7.62	184.92	4.52	0.03
y~s(SA200)+s(slope) +s(depth)	0.75	7.35	185.85	5.73	0.02
y~s(SA125_55)+s(depth)	0.75	6.94	185.43	5.83	0.02
y~s(SA200)+s(depth)	0.74	6.69	186.32	6.99	0.01
y~s(SA125)+s(depth)	0.74	6.53	186.25	7.45	0.01
y~s(SA125_55)+s(slope)	0.71	6.27	186.51	8.31	0.00
y~s(SA125)+s(slope)	0.71	5.93	187.19	9.65	0.00
y~s(SA125_55)+s(roughness)	0.70	5.78	187.26	10.06	0.00
y~s(SA125)+s(roughness)	0.70	5.48	187.89	11.27	0.00
y~s(SA200)+s(slope)	0.68	5.04	188.97	13.12	0.00
y~s(SA200_55)+s(slope)	0.68	4.80	189.46	14.06	0.00
y~s(SA455_55)+s(depth)	0.73	4.75	189.35	14.17	0.00

(Continued)

10.3389/fmars.2023.1208262

TABLE 1 Continued

Model	AUC	Deviance Explained	REML	ΔAIC	wAIC
y~s(SA200)+s(roughness)	0.66	4.54	189.77	14.94	0.00
y~s(SA455_55)+s(slope)	0.71	4.39	189.86	15.43	0.00
y~s(SA200_55)+s(roughness)	0.66	4.27	190.34	16.04	0.00
y~s(SA455_55)+s(roughness)	0.70	4.00	190.39	16.74	0.00

model fit for the best model (Supplementary Material Figure 1).

Opportunistic whale sightings

A total of 2,571 opportunistic sightings were recorded in January and February between 2015 and 2019 by CONAF, including 1,745 fin whale sightings (67.9% of total), 588 blue whale sightings (22.9% of total) and 238 humpback whale sightings (9.3% of total). No other whale species were sighted. Fin whale presence dominated during all years compared with blue and humpback whales, with a much higher average over the 5 years of data (Figure 5). Regarding monthly presence, the years with least fin whale presence were 2018 and 2019 (particularly in February) and with lowest blue whale presence was 2018 (both in January and February) and 2019 (particularly in February) (Figure 5). For humpback whales, no sightings were reported in 2018 and only two days with presence were recorded in 2019. The low overall whale presence in February 2019 was also reflected by low systematic sightings in 2019. Additionally, odontocete species were reported: bottlenose dolphins were the most common due to resident and transient populations in this area (Santos Carvallo et al., 2015; Pérez-Alvarez et al., 2018); Sperm whales (*Physeter macrocephalus*), pilot whales, Risso's dolphins, Dusky dolphins (*Lagenorhynchus obscurus*), and orca (*Orcinus orca*) were also sighted.

Oceanographic data

Local current measurements (Figures 6, 7) and hydrography (Figure 7) from 2008 show recirculation around the island and within the canyon. Figures 6, 7B show southward flow around the Isla Chañaral especially in the northern part of the channel between the island and the mainland. However, the southern transect (Figures 7D–F) across the southern part of the canyon reveals northerly flow along the western bank of the canyon (towards the left hand side of Figure 7E), while southerly flow persists on the eastern bank of the canyon (towards the right hand side of Figure 7E). In the southern section of the canyon, we observe colder, higher salinity, higher density water along the bottom of the canyon intruding upwards, indicated by upward bending temperature, salinity, and density isolines (Figures 7J–L). Based on the remote sensing data, spring 2017 was markedly cooler and more productive than spring 2018 (Figure 8), with the area of high Chla extending further offshore in 2017 (Figure 8C) compared to 2018 (Figure 8D). Note that spring 2017 and summer 2018 were under La Niña conditions,

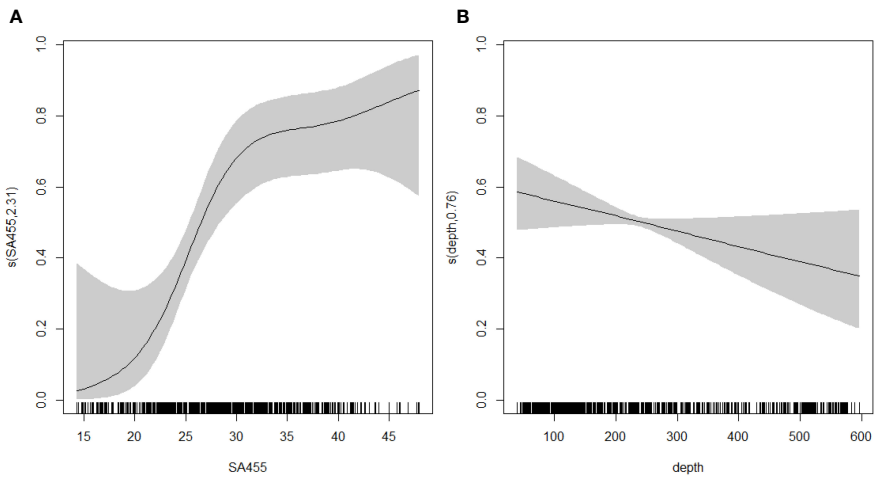

FIGURE 4
Response curves for the selected GAM with **(A)** 455kHz backscatter, and **(B)** depth as explanatory variables. Grey shades represent confidence intervals.

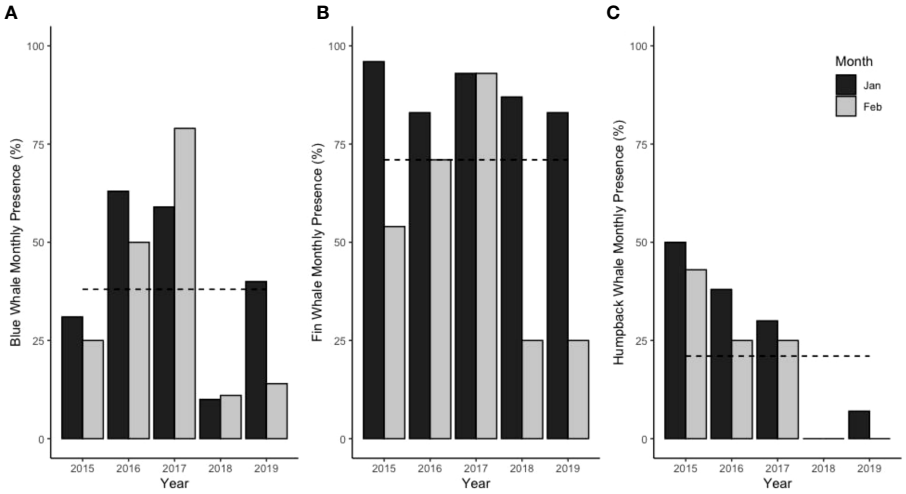

FIGURE 5
Monthly presence of whales in January and February as percentage of days with presence per month using opportunistic sighting data of **(A)** blue whales, **(B)** fin whales and **(C)** humpback whales. Dotted line indicates average over 5 years.

while spring 2018 and summer 2019 were under El Niño conditions (see Oceanic Niño Index, https://origin.cpc.ncep.noaa.gov/products/analysis_monitoring/ensostuff/ONI_v5.php).

Average geostrophic currents near the coast for both survey years showed different patterns, especially south of Isla Chañaral (Figures 9A, B). In summer 2018, currents near the coast flowed towards the coast generating a flow towards Isla Chañaral and the

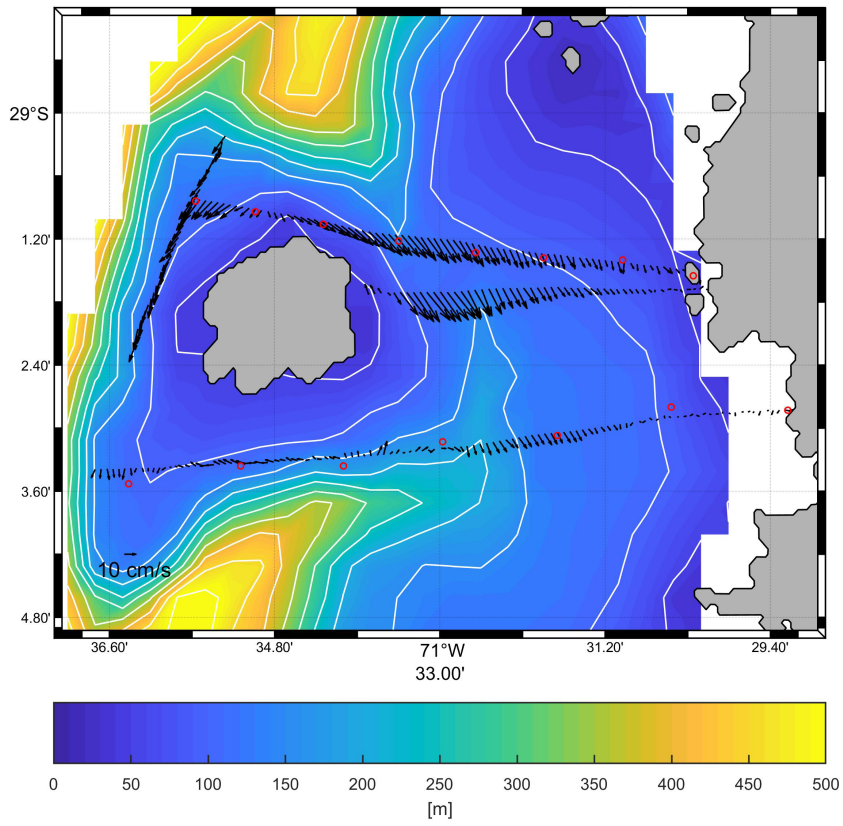

FIGURE 6
Surface current measurements around Isla Chañaral carried out on January 23, 2008 (Fisheries Research Fund grant: FIP 2006-56, 2008), over bathymetry from this study. Current vectors (black arrows) represent the vertical averages of current velocities (from a towed Acoustic Doppler Current Profiler, ADCP) over four transects. The red circles are the positions of the hydrographic (CTD) sampling stations north and south of Isla Chañaral. The cross-sections of the currents and hydrography are shown in Figure 9.

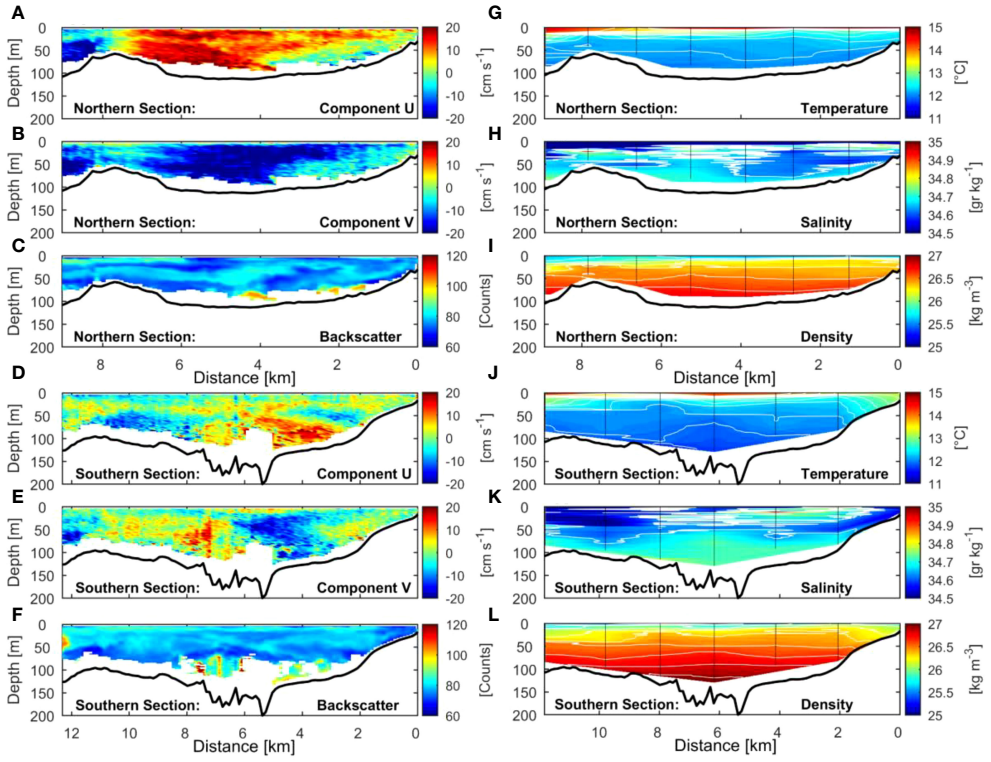

FIGURE 7
Cross-sections of the current velocities and hydrography around Isla Chañaral during January 23, 2008 (see Figure 6 for locations). **(A–C)** U (East-West) and V (North-South) components of the current velocities, and backscatter (from ADCP) for the northern section, respectively. **(D–F)** same as above but for the southern section. **(G–I)** Temperature, salinity and density (from the CTD) for the northern section, respectively. **(J–L)** same as previous, but for the southern section.

Humboldt Archipelago; while in summer 2019, the currents to the south of Isla Chañaral flowed away from the coast. However, very close to shore, in the channel between Isla Chañaral and the mainland, we observed flow to the southeast during both years (Figures 9A, B) which is in line with southward flow reported in Figures 6, 7B. Backscatter was highest over the canyon as seen in both northern and southern transects, and the edge of the continental shelf (Figures 7C, F).

The long-term average of the geostrophic currents off central-northern Chile (Figures 9C, D) showed a recirculation system between 28° and 31°S, with a flow towards the coast in the northern part of that region. This is also consistent with the average geostrophic flows from Isla Chañaral to the north during both surveys (Figures 9A, B).

Discussion

Our results highlight areas of higher backscatter and whale sightings around Isla Chañaral and the submarine canyon; and greater presence of whales and higher backscatter associated with bathymetric features (depth, slope and roughness). There is however, significant variation year-to-year in the presence of whales, as seen in both the systematic and opportunistic sighting datasets, driven by variation in oceanographic conditions. Here we discuss the circulation regime around Isla Chañaral and the Humboldt Archipelago which we summarize in a conceptual schema in Figure 10. We also discuss the dynamics of whales and prey around Isla Chañaral, and make some recommendations for protection of this habitat.

Circulation regime around the Humboldt Archipelago

The long-term average geostrophic currents over almost three decades revealed a recirculation system between 28° and 31°S showing flow back toward the coast in the northern part of that area. This recirculation could be part of a near zonal (east-west) pattern of the average geostrophic currents along the Chilean coast that is associated with so-called striations (Figure 10), i.e., bands interspersed with positive and negative zonal flows (Belmadani et al., 2017). These striations have been observed in different regions of the global ocean through remote-sensing altimetry and derived geostrophic currents (e.g., Maximenko et al., 2005; Belmadani et al., 2017). The presence of eastward and westward jets seems to result from the eddy field generated in the presence of planetary vorticity gradient and they efficiently develop near eastern boundaries related to particular coastal features (Davis et al., 2014; Belmadani et al., 2017). This circulation pattern may explain the high biological productivity in the area because productivity gets trapped nearer the coast in the Humboldt Archipelago area.

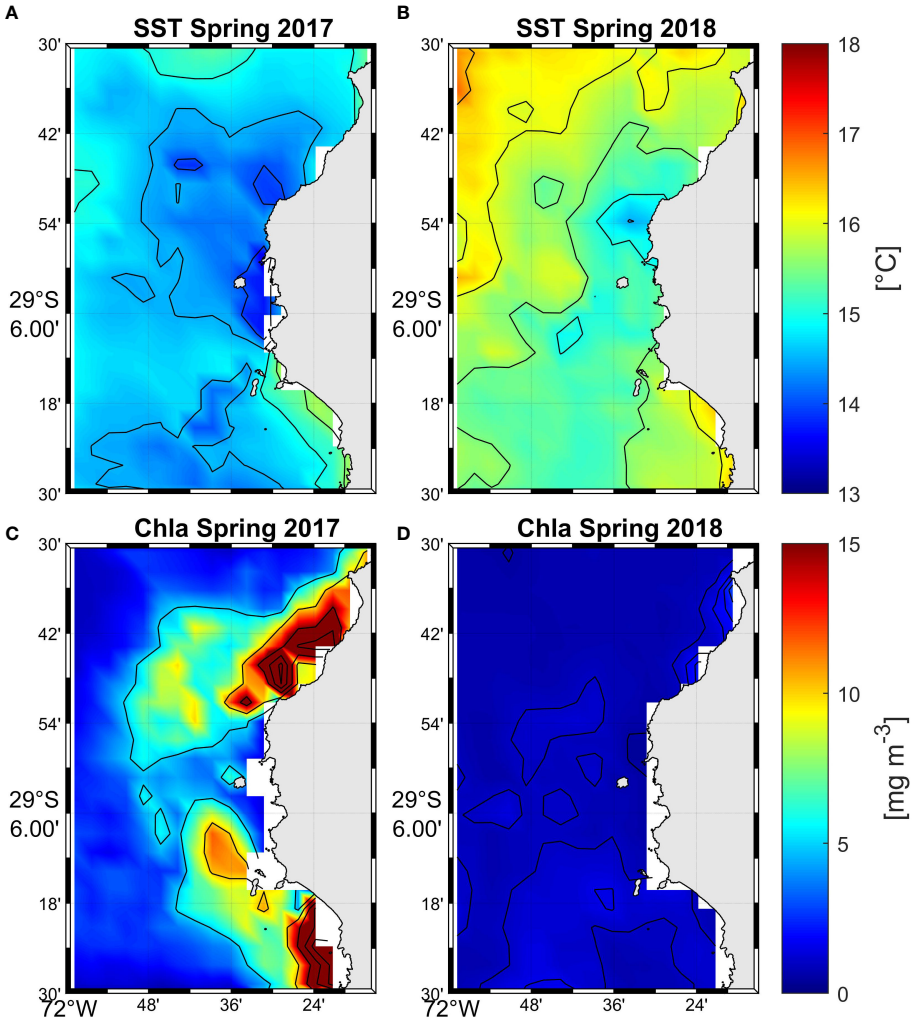

FIGURE 8
Mean sea surface temperature (top panels **A**, **B**) (°C) and chlorophyll a (bottom panels **C**, **D**) (mg m^{-3}) during spring (November) 2017 and 2018.

In the northern part of this study area we observed the mean geostrophic flow towards the coast (with an eastern component) (Figure 10) which should favor the transport of planktonic organisms towards the coast, especially those species that display diel vertical migration below of the superficial Ekman layer, like euphausiids, taking advantage of the opposite flow at depth. In general, selective vertical migration whether diel, seasonal or ontogenetic helps the species to conserve energy, locate food, retain a certain location or to move to other locations (e.g., Kämpf and Chapman, 2016). A recent study about lateral transport of zooplankton explains trophic and taxonomic similarities over the zonal gradient of central Chile showing the importance of geostrophic current on the zooplankton distribution and suggesting that cross-shelf advection is a key process promoting zooplankton export to the deep-water ecosystem (González et al., 2023). Although this study focused on offshore transport over a short observation period and did not consider the onshore component of transport, its results could show offshore zonal flow as part of the oceanic striations reported along the coast for long-term average flows, but without considering the onshore transport reported here. This onshore flow could in part explain why this area is so biologically productive and biodiverse and provides a good feeding habitat for whales that feed on euphausiids. During our study period, there was however variability in the flow of currents in the Humboldt Archipelago, mainly at south of Isla Chañaral i.e. 2018 the flow was toward coast and away from coast in 2019. This demonstrate interannual variability in the circulation regime around the Humboldt Archipelago, and may explain the low productivity, and consequently the low whale sightings observed that year.

Circulation around Isla Chañaral and the submarine canyon

Local current velocities measured in 2008 around Isla Chañaral clearly show the effects of the island and the submarine canyon on flow regime, with southeast flow coming from the northern part of the channel between the island and the mainland (Figure 10), which is consistent with the ADCP measurements made during this study.

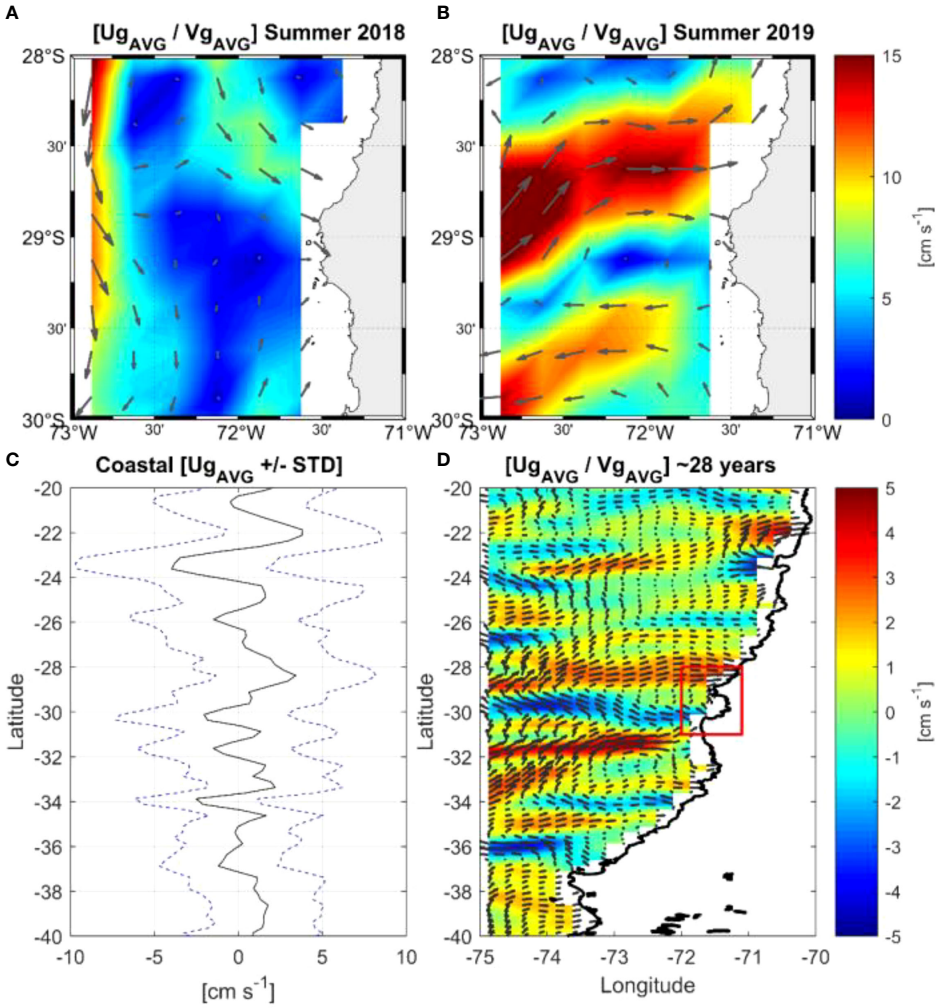

FIGURE 9
(Top panels **A**, **B**) Mean geostrophic currents during **(A)** January-February 2018, and **(B)** January-February 2019, respectively. In **(A, B)** the average velocity vectors located between Isla Chañaral and the mainland were obtained from an ADCP (Acoustic Doppler Current Profiler) deployed at a depth of 100 m. (Bottom panels **C**, **D**) Mean geostrophic currents over 28 years (1993-2020) in **(C)** for the most coastal pixel (+/- STD), and in **(D)** for the considered domain (20°-40°S), respectively. Note that in **(D)** the color shading is the velocity zonal component (Ug) to highlight the zonal flow (positive and negative) off the north-central zone of Chile. Red box contains the recirculation system that could explain the great biological productivity of the Humboldt Archipelago.

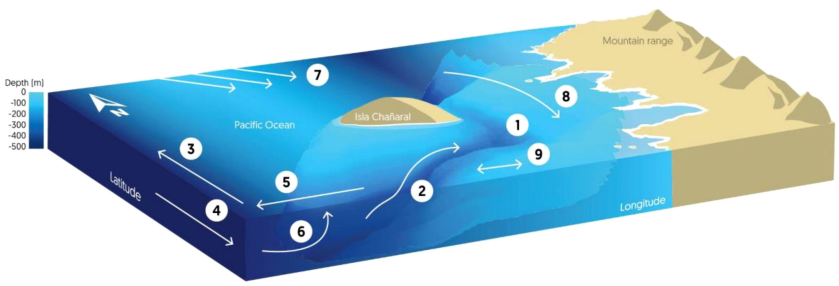

FIGURE 10
Scheme of the circulation and physical processes around Isla Chañaral: 1) Isla Chañaral Submarine Canyon, 2) Topographically caused upwelling associated with the canyon, 3) Upwelling Jet, 4) Peru-Chile Undercurrent (polewards), 5) Ekman Transport, 6) Coastal Upwelling, 7) Recirculation associated with zonal striations*, 8) Coastal circulation*, 9) Flow with changing direction. *Poorly understood connection between geostrophic flow and coastal circulation.

The intrusion of colder, more saline, denser bottom water (elevations of the temperature, salinity, and density isolines) into the southern part of submarine canyon suggests the entrance of locally upwelled water into the canyon from the south.

The geostrophic currents closest to the coast in the northern part of the island show a similar flow towards the coast for both measured periods (2018 and 2019) and for the long-term average. We hypothesize that this southeastward flow (towards the coast) is the dominant flow to the north of the island, but more observations of currents in the region are needed to verify this. The currents to the south of the island are more complex and show a cyclonic rotation over the canyon. This has been reported in several studies on the hydrodynamic effects of canyons in EBUS (e.g., Hickey, 1997; Sobarzo et al., 2016; Saldías and Allen, 2020). The presence of canyons in the continental shelf produces a geostrophic flow imbalance along the isobaths because of the abrupt change in the bottom topography, generating ageostrophic flows transverse to the shelf within and over the canyon (Allen et al., 2001; Allen and Durrieu de Madron, 2009), inducing local upwelling and even cyclonic eddies (Klinck, 1996; Allen and Hickey, 2010; Ramos-Musalem and Allen, 2019), depending on the direction of regional flow and stratification. However, it is not clear whether the pattern of currents detected in the canyon is due solely to the presence of the canyon or is also caused by the joint effect of the canyon and the island; this requires a more detailed study of the currents in the zone. Despite the above, the pattern of currents in the region can explain the concentration of zooplankton around Isla Chañaral and in the canyon, as found for other canyons elsewhere (e.g., Allen et al., 2001; Allen et al., 2010).

Spatial distribution of whales and prey around Isla Chañaral

Based on both observations and studies of fecal plumes from whales around Isla Chañaral, we know that fin whales and blue whales feed exclusively on the euphausiid species *E. mucronata* in this area (Pérez et al., 2006; Buchan et al., 2021). *E. mucronata* is a keystone species in the HCS, and sustains higher trophic levels (Antezana, 2010) and is strongly associated with wind-driven coastal upwelling centers (Escribano et al., 2000). Planktonic prey like euphausiids are known to concentrate in areas where physical processes, such as the interaction between bathymetric and local circulation, promote their aggregation (e.g., Croll et al., 2005; Doniol-Valcroze et al., 2012). Our results indicate that the circulation regime in the wider Humboldt Archipelago area and the local circulation around Isla Chañaral and the submarine canyon, concentrate planktonic prey and therefore provide feeding habitat for baleen whales.

During the 2018 surveys, fin whales were spatially associated with the submarine canyon between Isla Chañaral and the mainland and the slope to the south of the canyon, features which are apparent in the bathymetric data presented here. Zooplankton backscatter was also highest in the canyon, as seen in the AZFP survey data from 2018 and the towed ADCP from 2008. The association of whales and their prey with bathymetric features and submarine canyons has been described before for blue whale feeding grounds, such as the Monterey Bay (Croll et al., 2005) and the St. Lawrence Gulf Estuary (Doniol-Valcroze et al., 2012), and has been suggested in Chilean Patagonia (Buchan and Quiñones, 2016). Complex bathymetry has a known effect on the aggregation of zooplankton (e.g., Croll et al., 2005) and retention of fish larval as described by Rojas and Landaeta (2014) for Mejillones Bay northern of Chile. A review of canyons in the California Current System (also an EBUS) by Santora et al. (2018) showed that 76% of krill hotspots occurred within or near submarine canyons, including smaller canyons (25 km^2) like the Isla Chañaral canyon. Allen et al. (2001) showed eddy formation at the head of a shelf-break canyon during an upwelling event that concentrated euphausiids; it is not clear if this mechanism also applies to a much smaller canyon like the Isla Chañaral canyon.

Spatial distribution of whales and backscatter was in line with the results of the GAMs, where higher presence was associated with shallower depths (like those found near-shore and in the canyon) and high backscatter, particularly in the 455 kHz and 200 kHz channels. Similarly, a distribution model of fin whales in the study area demonstrated that shallow depths was one of the variables that better explained the presence and habitat use of this species (Barilari, 2022). Future research should include further surveys and should examine the physical and biological dynamics of the submarine canyon, particularly the links between circulation and euphausiid density in space and time.

Interannual variation in whale presence and oceanographic conditions

Although opportunistic sightings of whales off Isla Chañaral have been consistent in the summer months since at least 2015, interannual variability is likely caused by interannual variation in oceanographic conditions and therefore prey availability for whales. In effect, February 2019 was a particularly poor year for fin whale sightings, as seen by both the systematic surveys and the CONAF opportunistic sighting data. The differences in geostrophic flow and remote-sensing oceanographic data can explain differences between 2018 and 2019, where geostrophic flow was towards the coast in summer 2018 and the summer of 2018 was preceded by a cooler and more productive spring (September to December 2017). In contrast, during summer 2019, geostrophic flow was away from the coast and a warmer and less productive spring preceded this summer. The low near-shore sightings of whales during 2019, due to the low-productivity conditions around Isla Chañaral, suggests that in years where productivity is low around Isla Chañaral, whales may move offshore. Offshore scientific surveys of fisheries during summer 2019 did in fact report offshore sightings of whales (Bedriñana-Romano et al., 2022).

Expansion of the Isla Chañaral marine reserve and implementation of the Humboldt Archipelago marine protected area

Isla Chañaral has become increasingly well known nationally and internationally as a feeding ground for baleen whales,

particularly fin whales, and an area where small-scale community-based whale-watching has flourished (Sepúlveda et al., 2018). The Humboldt Archipelago and Isla Chañaral is critical feeding habitat for fin, blue and humpback whales, and a host of other marine species, including marine birds and other marine mammals. Fin whales were the most hunted mysticete whales in the HCS (Aguayo-Lobo et al., 1998) and are considered Endangered by the Chilean Ministry of the Environment, as are blue whales and humpback whales (https://clasificacionespecies.mma.gob.cl/). Despite the recent population estimate for fin whales in the HCS of 2511.5 ind. (2.5-97.5% C.I. = 1387.9 – 5068.5) (Bedriñana-Romano et al., 2022) there is currently no information on the population trend of this species or the other baleen whales in the HCS, and thus no knowledge of whether these populations are recovering or not.

Given the unique oceanographic and bathymetric features that lead to high prey availability for baleen whales around Isla Chañaral, and also due to recent studies have shown that a large proportion of the sightings of cetacean species occur outside the current protected area (Sepúlveda et al., 2016, Gutiérrez et al. In press) we recommend that the Isla Chañaral Marine Reserve needs to be expanded. The Humboldt Archipelago has recently received international recognition as an Important Marine Mammal Area (IMMA) (https://www.marinemammalhabitat.org/portfolio-item/humboldt-archipelago-imma/). IMMAs are "*discrete portions of habitat, important to marine mammal species, that have the potential to be delineated and managed for conservation*". Also, during 2023 a MU MPA was approved by the Chilean Council of Ministers for Sustainability. This MPA could strengthen the conservation of marine mammals and their habitat, by including special zoning for critical features like the canyon described here. The protection of the canyon is likely to have benefits beyond the protection of critical habitat for whales, given the important ecosystem services provided by submarine canyons (Fernández-Arcaya et al., 2017). Lastly, we recommend that the MU MPA administration plan excludes the development of large industrial projects that lead to high levels of marine traffic and other environmental threats for whales and other species.

Conclusions

1) We observed overlapping spatial distribution of whales, backscatter and the submarine canyon that is located to the south of the island and in the channel between the island and the mainland. This is in line with whale presence being associated with high levels of backscatter and shallow depths according to the GAM analysis. Higher sightings in summer 2018 vs. summer 2019 coincided with higher backscatter, indicating that these differences in whale presence were likely driven by differences in prey availability.
2) In summer 2018, geostrophic flow towards the coast and a cold productive spring could explain high backscatter and whale sightings around Isla Chañaral. In summer 2019, geostrophic flow away from the coast and a warm spring with low productivity could explain low backscatter levels and whale sightings around Isla Chañaral, highlighting the interannual variability of the area.
3) Long-term average geostrophic currents form a recirculation system between 28°S and 31°S that could transport nutrient-rich upwelled surface waters back towards the Humboldt Archipelago and contribute to high biological productivity in this area.
4) The unique oceanographic features of the Isla Chañaral and the Humboldt Archipelago area contribute to successful foraging conditions for Endangered baleen whales. Based on this evidence, we recommend the expansion of the Isla Chañaral Marine Reserve to include the submarine canyon between the mainland and the island, and the implementation of a MU MPA for the entire Humboldt Archipelago area that explicitly protects this critical habitat from large industrial projects (including mega-ports and associated marine traffic routes).

Data availability statement

The raw data supporting the conclusions of this article will be made available by the authors, without undue reservation. Further inquiries can be directed to the corresponding author. Requests to access the datasets should be directed to jorge.oyanadel@ce.ucn.cl.

Ethics statement

Ethical approval was not required for the study involving animals in accordance with the local legislation and institutional requirements because no animals were manipulated and the regulations for sighting marine mammals established by the National Fisheries Service and Undersecretary of Fisheries of Chile (D.S. N° 38-2011) were strictly followed.

Author contributions

SB contributed to study conception, design, data collection and analysis, manuscript preparation, including writing the first draft of this manuscript, and securing funding. MR contributed to study design, oceanographic and hydroacoustic data collection and analysis, securing funding, and writing and preparation of manuscript. JO contributed to hydroacoustic data collection, processing and analysis, oceanographic data analysis, and writing and preparation of manuscript. MS contributed to sighting data collection and analysis, writing and preparation of manuscript. LB-R contributed to study design, sighting data collection and analysis, and writing and preparation of manuscript. MV contributed to acoustic data collection, processing and data analysis. MM carried out CONAF sighting data collection. OA contributed to processing

and analysis of satellite data. MS and CO contributed to study design, manuscript preparation and securing funding. SP contributed to acoustic data collection, processing and analysis. All authors contributed to the article and approved the submitted version.

Funding

The author(s) declare financial support was received for the research, authorship, and/or publication of this article. Financial support was provided by Agencia Nacional de Investigación y Desarrollo (ANID) grant R16A10003 to CO and SB. Partial funding was provided by Centro COPAS Sur-Austral (ANID PFB31 and ANID AFB170006), and Centro COPAS Coastal (ANID FB210021). This study was also made possible with an Early Career Scientist award to SB from ASL Environmental Sciences. Support was also provided by ANID project ANILLO ATE220044 (BiodUCCT) awarded to MR and FONDECYT project #11190999 awarded to OA, also OA, SB, CO, MR and MV are grateful for ANID's funding through the R20F0008 CLAP project. We thank the Fisheries Research Fund FIP 2006-56 for auxiliary oceanographic data. All instrument deployments were carried out under SHOA resolutions 13270-24-74, 13270-24-136, 13270-24-137, 13270-24-155, 13270-24-161. A MATLAB, 2022a Academic License to the Universidad Católica del Norte was used in this research.

Acknowledgments

Our thanks to our captains Rafael González and Rafael González Jr. The authors thank Dr. Ricardo Bravo for help with analysis of zooplankton samples. Our thanks to the entire fleet of community whale-watching adventure tourism vessels that report opportunistic sighting data on a daily basis and the Corporación Nacional Forestal (CONAF) Atacama and their team of park rangers for collecting and compiling the opportunistic sighting data. Our thanks to Dr. Ana Ventero for help with acoustic data analysis and, finally, to all the anonymous reviewers.

Conflict of interest

The authors declare that the research was conducted in the absence of any commercial or financial relationships that could be construed as a potential conflict of interest.

Publisher's note

Supplementary material

The Supplementary Material for this article can be found online at: https://www.frontiersin.org/articles/10.3389/fmars.2023.1208262/full#supplementary-material

SUPPLEMENTARY FIGURE 1
Results for simulation-based and scaled residuals diagnostics for model-fit assessment on the best model retaining SA455 and depth. Left top panel shows expected versus observed residual plot using scaled residuals. Top right panel shows residual dispersion for observed data (red line) and simulated data (histogram). Left bottom panel show quantile deviation test, indicating no deviations detected. Right bottom panel shows result for outlier test, indicating now significant outliers detected.

References

Aguayo-Lobo, A., Torres., D., and Acevedo., J. (1998). Los mamíferos marinos de Chile. *Serie Científica. INACH* 48 (January), 19–159.

Akaike, H. (1973). *Information theory and an extension of the maximum likelihood principle*. Eds. B. N. Petrov and F. Csaki (Akademiai Kiado, Budapest: Proceedings of the 2nd International Symposium on Information Theory), 267–281.

Allen, S. E., and Durrieu de Madron, X. (2009). A review of the role of submarine canyons in deep-ocean exchange with the shelf. *Ocean Sci.* 5 (4), 607–620. doi: 10.5194/os-5-607-2009

Allen, S. E., and Hickey, B. (2010). Dynamics of advection-driven upwelling over a shelf break submarine canyon. *J. Geophysical Res.* 115 (C8). doi: 10.1029/2009JC005731

Allen, S. E., Vindeirinho, C., Thomson, R., Foreman, M. G., and Mackas, D. (2001). Physical and biological processes over a submarine canyon during an upwelling event. *Can. J. Fisheries Aquat. Sci.* 58 (4), 671–684. doi: 10.1139/f01-008

Antezana, T. (2010). Euphausia mucronata: A keystone herbivore and prey of the Humboldt Current System. *Deep Sea Res. Part II: Topical Stud. Oceanography* 57 (7–8), 652–662. doi: 10.1016/j.dsr2.2009.10.014

ASL. (2017). *AZFP (Acoustic Zooplankton Fish Profiler) operator's manual* (Victoria, Canada: ASL Editor Environmental Sciences Inc.), 108.

Barilari, F. (2022). *Distribución potencial de la ballena fin (Balaenoptera physalus) en la zona norte y centro de Chile* (Universidad de Valparaíso: Tesis de Magister en Ciencias Biológicas mención Biodiversidad y Conservación).

Barlow, D. R., Klinck, H., Ponirakis, D. W., Garvey, C., and Torres, L.G. (2021). Fashionably late: Temporal and spatial lags between wind and blue whales in a coastal upwelling system. *Sci. Rep.* 1–10. doi: 10.1038/s41598-021-86403-y

Bedriñana-Romano, L., Zarate, P. M., Hucke-Gaete, R., Viddi, F. A., Buchan, S. J., Cari, I., et al. (2022). Abundance and distribution patterns of cetaceans and their overlap with vessel traffic in the Humboldt Current Ecosystem, Chile. *Sci. Rep.* 12 (1), 1–15. doi: 10.1038/s41598-022-14465-7

Belmadani, A., Concha, E., Donoso, D., Chaigneau, A., Colas, F., Maximenko, N., et al. (2017). Striations and preferred eddy tracks triggered by topographic steering of the background flow in the eastern South Pacific. *J. Geophysical Research: Oceans* 122 (4), 2847–2870. doi: 10.1002/2016JC012348

Boltovskoy, D. (1981). *Radiolaria: en Atlas del zooplancton del Atlántico Sudoccidental y métodos de trabajo con el zooplancton marino* (Mar del Plata, Argentina: Mar del Plata: Instituto Nacional de Investigación y Desarrollo Pesquero INIDEP), 261–316.

Buchan, S. J., Gutiérrez, L., Baumgartner, M. F., Stafford, K. M., Ramirez, N., Pizarro, O., et al. (2022). Distribution of blue and sei whale vocalizations, and temperature - salinity characteristics from glider surveys in the Northern Chilean Patagonia mega-estuarine system. *Front. Mar. Sci.* 9. doi: 10.3389/fmars.2022.903964

Buchan, S. J., and Quiñones, R. A. (2016). First insights into the oceanographic characteristics of a blue whale feeding ground in northern Patagonia, Chile. *Mar. Ecol. Prog. Ser.* 554, 183–199. doi: 10.3354/meps11762}

Buchan, S. J., Vásquez, P., Olavarría, C., and Castro, L. R. (2021). Prey items of baleen whale species off the coast of Chile from fecal plume analysis. *Mar. Mammal Sci.* 37 (3), 1116–1127. doi: 10.1111/mms.12782

Cox, S., Embling, C. B., Hosegood, P. J., Votier, S. C., and Ingram, S. N. (2018). Oceanographic drivers of marine mammal and seabird habitat-use across shelf-seas: a guide to key features and recommendations for future research and conservation management. *Estuarine Coast. Shelf Sci.* 212, 294–310. doi: 10.1016/j.ecss.2018.06.022

Croll, D., Marinovic, B., Benson, S., Chavez, F., Black, N., Ternullo, R., et al. (2005). From wind to whales: trophic links in a coastal upwelling system. *Mar. Ecol. Prog. Ser.* 289, 117–130. doi: 10.3354/meps289117

Daneri, G., Dellarossa, V., Quiñones, R., Jacob, B., Montero, P., and Ulloa, O. (2000). Primary production and community respiration in the Humboldt Current System off Chile and associated oceanic areas. *Mar. Ecol. Prog. Ser.* 197, 41–49. doi: 10.3354/meps197041

Davis, A., di Lorenzo, E., Luo, H., Belmadani, A., Maximenko, N., Melnichenko, O., et al. (2014). Mechanisms for the emergence of ocean striations in the North Pacific. *Geophysical Res. Lett.* 41 (3), 948–953. doi: 10.1002/2013GL057956

de Robertis, A., and Higginbottom, I. (2007). A post-processing technique to estimate the signal-to-noise ratio and remove echosounder background noise. *ICES J. Mar. Sci.* 64 (6), 1282–1291. doi: 10.1093/icesjms/fsm112

Doniol-Valcroze, T., Berteaux, D., Larouche, P., and Sears, R. (2007). Influence of thermal fronts on habitat selection by four rorqual whale species in the Gulf of St. Lawrence. *Mar. Ecol. Prog. Ser.* 335, 207–216. doi: 10.3354/meps335207

Doniol-Valcroze, T., Lesage, V., Giard, J., and Michaud, R. (2012). Challenges in marine mammal habitat modelling: Evidence of multiple foraging habitats from the identification of feeding events in blue whales. *Endangered Species Res.* 17 (3), 255–268. doi: 10.3354/esr00427

Escribano, R., Marin, V. H., and Irribarren, C. (2000). Distribution of Euphausia mucronata at the upwelling area of Peninsula Mejillones , northern Chile: the influence of the oxygen minimum layer. *Scientia Marina* 64 (1), 69–77. doi: 10.3989/scimar.2000.64n169

Fernández-Arcaya, U., Ramírez-Llodra, E., Aguzzi, J., Allcock, A. L., Davies, J. S., Dissanayake, A., et al. (2017). Ecological role of submarine canyons and need for canyon conservation: a review. *Front. Mar. Sci.* 4. doi: 10.3389/fmars.2017.00005

Gaymer, C. F., Stotz, W., Garay Flühmann, R., Luna-Jorquera, G., and Ramos, M. (2008). *Evaluación de línea base de Las Reservas Marinas "Isla Chañaral" e "Isla Choros-Damas"* (Informe Final Proyecto FIP 2006-56, Subsecretaría de Pesca, Chile), 532.

González, C. E., Bode, A., Fernández-Urruzola, I., Hidalgo, P., Oerder, V., and Escribano, R. (2023). The lateral transport of zooplankton explains trophic and taxonomic similarities over the zonal gradient of central Chile. *J. Mar. Syst.* 238, 103840. doi: 10.1016/j.jmarsys.2022.103840

Gutiérrez, E., Letelier, L., Santos-Carvallo, M., Barilari, F., Gutiérrez, L., Pérez-Alvarez, M. J., et al. Zoning proposal for a Marine Protected Area in Chile: a conservation tool for large cetaceans. *Ocean Coast. Management.* [Epub ahead of print].

Harris, R., Wiebe, P., Lenz, J., Skjoldal, H. R., and Huntley, M. (2000). *ICES Zooplankton methodology manual* (London: Academic Press).

Hartig, F. (2022). *DHARMa: residual diagnostics for hierarchical (Multi-level / mixed) regression models.*

Hickey, B. (1997). The response of a steep-sided, narrow canyon to time-variable wind forcing. *J. Phys. Oceanography* 27 (5), 697–726. doi: 10.1175/1520-0485(1997)027<0697:TROASS>2.0.CO;2

Hijmans, R. J., van Etten, J., Cheng, J., Sumner, M., Mattiuzzi, M., and Greenberg, J. A. (2018). *Raster: geographic data analysis and modeling.*

Joyce, T. M. (1989). On in *situ* "calibration" of shipboard ADCPs. *J. Atmospheric Oceanic Technol.* 6, 169–172. doi: 10.1175/1520-0426(1989)006<0169:OISOSA>2.0.CO;2

Kämpf, J., and Chapman, P. (2016). *Upwelling systems of the world A scientific journey to the most productive marine Ecosystems* (Switzerland: Springer International Publishing), 443.

Klinck, J. (1996). Circulation near submarine canyons: A modeling study. *J. Geophysical Res.* 101 (C1), 1211–1223. doi: 10.1029/95JC02901

Largier, J. L. (2020). Upwelling bays: How coastal upwelling controls circulation, habitat and productivity in bays. *Annu. Rev. of Mar. Sci.* 12, 415–447. doi: 10.1146/annurev-marine-010419-011020

MacLennan, D. N., Fernandes, P. G., and Dalen, J. (2002). A consistent approach to definitions and symbols in fisheries acoustics. *ICES J. Mar. Sci.* 59 (2), 365–369. doi: 10.1006/jmsc.2001.1158

Marra, G., and Wood, S. N. (2011). Practical variable selection for generalized additive models. *Comput. Stat Data Anal.* 55 (7), 2372–2387. doi: 10.1016/j.csda.2011.02.004

Maximenko, N. A., Bang, B., and Sasaki, H. (2005). Observational evidence of alternating zonal jets in the world ocean. *Geophysical Res. Lett.* 32 (12). doi: 10.1029/2005GL022728

Montecino, V., and Lange, C. B. (2009). The Humboldt Current System: Ecosystem components and processes, fisheries, and sediment studies. *Prog. Oceanography* 83 (1–4), 65–79. doi: 10.1016/j.pocean.2009.07.041

Monteiro, P., Dewitte, B., Scranton, M., Palmier, A., and van der Plas, A. K. (2011). The role of open ocean boundary forcing on seasonal to decadal-scale variability and long-term change of natural shelf hypoxia. *Environ. Res. Letters.* 6, 25002. doi: 10.1088/1748-9326/6/2/025002

Moraga, J., Valle-Levinson, A., Ramos, M., and Pizarro, M. (2011). Upwelling-triggered near-geostrophic recirculation in an equatorward facing embayment. *Continental Shelf Res.* 31, 1991–1999. doi: 10.1016/j.csr.2011.10.002

Palma, S., and Kaiser, K. (1993). *Plancton marino de aguas Chilenas* (Chile: Ediciones Universitarias de Valparaíso, Universidad Católica de Valparaíso), 151.

Pérez, M. J., Thomas, F., Uribe, F., Sepúlveda, M., Flores, M., and Moraga, R. (2006). Fin Whales (Balaenoptera physalus) Feeding on Euphausia mucronate in Nearshore Waters off North-Central Chile. *Aquat. Mammals* 32 (1), 109–113. doi: 10.1578/am.32.1.2006.109

Pérez-Alvarez, M. J., Vásquez, R. A., Moraga, R., Santos-Carvallo, M., Kraft, S., Sabaj, V., et al. (2018). Home sweet home: social dynamics and genetic variation of a long-term resident bottlenose dolphin population off the Chilean coast. *Anim. Behav.* 139, 81–89. doi: 10.1016/j.anbehav.2018.03.009

Ramos-Musalem, K., and Allen, S. E. (2019). The impact of locally-enhanced vertical diffusivity on the cross-shelf transport of tracers induced by a submarine canyon. *J. Phys. Oceanography* 49, 561–584. doi: 10.1175/jpo-d-18-0174.1

Redfern, J., Moore, T. J., Fiedler, P. C., de Vos, A., Brownell, R. L. Jr., Forney, K. A., et al. (2017). Predicting cetacean distributions in data-poor marine ecosystems. *Diversity Distributions* 23 (4), 394–408. doi: 10.1111/ddi.12537

Roberts, J. J., Best, B. D., Mannocci, L., Fujioka, E., Halpin, P. N., Palka, D. L., et al. (2016). Habitat-based cetacean density models for the U.S. Atlantic and Gulf of Mexico. *Sci. Rep.* 6 (1), 22615. doi: 10.1038/srep22615

Rojas, P. M., and Landaeta, M. F. (2014). Fish larvae retention linked to abrupt bathymetry at Mejillones Bay (northern Chile) during coastal upwelling events. *Latin Am. J. Aquat. Res.* 42, 989–1008. doi: 10.3856/vol42-issue5-fulltext-6

Rutllant, J., and Montecinos, V. (2002). Multiscale upwelling forcing cycles and biological response off north-central Chile. *Rev. Chil. Hist. Natural* 75, 231. doi: 10.4067/S0716-078X2002000100020

Saldías, G. S., and Allen, S. E. (2020). The influence of a submarine canyon on the circulation and cross-shore exchanges around an upwelling front. *J. Phys. Oceanography* 50 (6), 1677–1698. doi: 10.1175/jpo-d-19-0130.1

Santora, J. A., Zeno, R., Dorman, J. G., and Sydeman, W. J. (2018). Submarine canyons represent an essential habitat network for krill hotspots in a Large Marine Ecosystem. *Sci. Rep.* 8 (1), 7579. doi: 10.1038/s41598-018-25742-9

Santos Carvallo, M., Pérez Alvarez, M. J., Muniain, V., Moraga, R., Oliva, D., and Sepúlveda, M. (2015). Trophic niche overlap between sympatric resident and transient populations of bottlenose dolphins in the Humboldt Current System off north-central Chile. *Mar. Mammal Science.* 31 (2), 790–799. doi: 10.1111/mms.12185

Sepúlveda, M., Oliva, D., Pavez, G., and Santos-Carvallo, M. (2016). *Caleta Chañaral de Aceituno: Destino turístico de alta calidad para el avistamiento de cetáceos, otros mamíferos y aves marinas* (Chile: Servicio Nacional de Pesca y Acuicultura).

Sepúlveda, M., Pérez-Álvarez, M. J., Santos-Carvallo, M., Pavez, G., Olavarría, C., Moraga, R., et al. (2018). From whaling to whale watching: Identifying fin whale critical foraging habitats off the Chilean coast. *Aquat. Conserv. Mar. Freshw. Ecosystem* 28 (4), 821–829. doi: 10.1002/aqc.2899

Shaffer, G., Hormázabal, S., Pizarro, O., and Salinas, S. (1999). Seasonal and interannual variability of currents and temperature off central Chile. *J. Geophysical Research: Oceans.* 104, 29951–29961. doi: 10.1029/1999JC900253

Sing, T., Sander, O., Beerenwinkel, N., and Lengauer, T. (2005). ROCR: visualizing classifier performance in R. *Bioinformatics* 21 (20), 3940–3941. doi: 10.1093/bioinformatics/bti623

Sobarzo, M., Saldías, G. S., Tapia, F. J., Bravo, L., Moffat, C., and Largier, J. L. (2016). On subsurface cooling associated with the Biobio River canyon (Chile). *J. Geophysical Research: Oceans* 121, 4568–4584. doi: 10.1002/2016JC011796

Thiel, M., Macaya, E., Acuña, E., Amtz, E., Bastías, H., Brokordt, K., et al. (2007). The Humboldt current system of northern and central Chile: Oceanographic processes, ecological interactions and socio-economic feedback. *Oceanography Mar. Biology: Annu. Rev.* 45, 195–344. doi: 10.1201/9781420050943

Toro, F., Vilina, Y. A., Capella, J. J., and Gibbons, J. (2016). Novel coastal feeding area for eastern South Pacific fin whales (Balaenoptera physalus) in mid-latitude humboldt current waters off Chile. *Aquat. Mammals* 42 (1), 47–55. doi: 10.1578/AM.42.1.2016.47

Valle-Levinson, A., and Moraga-Opazo, J. (2006). Bipolar residual circulation in two equatorward facing bays. *Continental Shelf Res.* 26, 179–193. doi: 10.1016/j.csr.2005.10.002

Ventero, A. (2016). *Estudio biológico de la capa de dispersión acústica estival en el mar de Alborán y su implicación en la evaluación de pelágicos costeros* (Doctoral dissertation, Universitat de les Illes Balears).

Ventero, A., Iglesias, M., and Córdoba, P. (2019). Krill spatial distribution in the Spanish Mediterranean Sea in summer time. *J. Plankton Res.* 41 (4), 491–505. doi: 10.1093/plankt/fbz030

Wood, S. N. (2017). *Generalized additive models: an introduction with R, 2nd ed.* (Boca Raton, USA: CRC Press).